

# A reaction-diffusion model for the hydration of calciumsulphate (gypsum) and microstructure percolation.

F. Tzschichholz<sup>1</sup> and H. J. Herrmann<sup>1</sup>

<sup>1</sup> *Institut für Computeranwendungen I, Universität Stuttgart,  
Pfaffenwaldring 27, D-70569 Stuttgart, Germany*

(March 22, 2002)

We have numerically investigated a reaction-diffusion model for the hydration of calciumsulphate (gypsum). The simulations were conducted for two and three dimensional systems. While the dissolution of anhydrous gypsum is considered irreversible at a finite rate the precipitation/dissolution reaction for the calciumdihydrate is considered reversible. The latter reaction is assumed to be controlled by the dihydrate's equilibrium solubility *and* the ability of the system to react on supersaturation only at a certain velocity described by the reaction rate constant of precipitation. For  $d = 2$  we find at early times an accelerated hydration period followed by a maximum and a decreasing hydration rate. For large times the ionic product of involved species assumes closely the value of the di-hydrate equilibrium solubility. Calculated model micro-structures exhibit typical features such as inner and outer hydrate products, induction and dormant period as well as bridging. Furthermore we find that the overall chemical reactivity as a function of initial anhydrous (volume) concentration  $p$  exhibits a maximum close to the percolation point of the underlying lattice. Employing a rescaling procedure we find *two* percolation thresholds in  $d = 2$ ,  $p_c^{min} = 0.44 \pm 0.015$  and  $p_c^{max} = 0.77 \pm 0.02$ , for the initial anhydrous gypsum concentration *between* which percolating dihydrate structures can be attained. For  $d = 3$  we find  $p_c^{min} = 0.10 \pm 0.02$  and  $p_c^{max} = 0.95 \pm 0.02$ .

PACS number(s): 61.43.-j, 81.35.+k, 81.30.Mh

## I. INTRODUCTION

Gypsum is perhaps one of the oldest crafting and building materials human kind has cultivated beside wood, iron, and stone. There exists a long tradition of using this material in arts, medicine, paleontology, archeology, as well as a light-weighted building material. Its widespread use is likely due to its natural abundance, its almost total flexibility in applications, its chemical inertness and certainly its low costs. For an overview of the various applications we refer the interested reader to the survey of Wirsching [1]

Gypsum belongs to the group of calcium-sulphates with its various hydrates. A material class exhibiting some common phenomenological properties are the calcium-silicates, mostly termed as cementious materials. Cementious materials are, however, of much higher intrinsic strength than gypsum due to their chemical shrinkage and are therefore in technical applications mostly preferred to gypsum. While most cementious materials do precipitate as a gelatinous phase, calcium-sulphates appear always in crystalline modifications (needles).

Both calcium-sulphates as well as calcium-silicates are already well characterized on a molecular level [2,3]. However, it appears to us that gypsum is less understood compared to calcium-silicates on the macroscopic scale. For more recent experimental investigations we refer the interested reader to Ref. 4. For cementious materials microstructure computer models have been recently developed [5–8]. Though the cementious systems are much more complex from a chemical point of view their huge economical importance as the building material of choice has focussed the attention on the modeller's side. In the

on diffusion-reaction calculations. In the practice, the most important feature of the setting of gypsum is the formation of rigid structure of the hydrates. The necessary condition for this to occur is a connected structure, in other words, that the hydrate aggregate percolates. In this paper we will therefore investigate under which conditions (concentration of a hydrate) the end product of the reaction forms a percolating cluster.

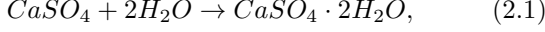
## II. PHYSICOCHEMICAL ASPECTS

The hydration of anhydrous calciumsulphate,  $CaSO_4$  - in the following *CS*, is based on dissolution/precipitation reactions forming various calcium-sulfohydrates [1]. The hydrates,  $CaSO_4 \cdot n H_2O$ , are distinguished by the molar amount  $n$  of bound crystal-water. In connection with the amount of physically bound water one observes different physico-chemical properties as for example crystal-symmetries, densities, or solubilities. The two most important hydrates are the semihydrate,  $n = 1/2$ , and the dihydrate,  $n = 2$ . There are two 'modifications' of the semihydrate called the  $\alpha$ - and  $\beta$ -semihydrate. On the side of the anhydrous calciumsulphates three forms are distinguished: soluble CS (A III), dead CS (A II), and high temperature CS (A I). Typical solubilities at room temperature and normal pressure are *2 gramm/liter* for the dihydrate, *2.5 gramm/liter* for A II, *5.8 gramm/liter* for  $\alpha$ -semihydrate, and *7.6 gramm/liter* for  $\beta$ -semihydrate. The solubilities for  $\alpha$ -,  $\beta$ -semihydrate and A II decrease monotonically with increasing temperature while the dihydrate exhibits a flat maximum at temperatures

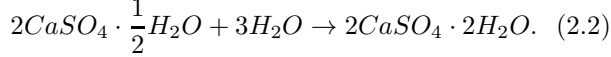
which consists almost only of dihydrate, b) anhydrous stone consisting almost only of A II, and c) technological mixing forms consisting mostly of A II and A III and semihydrates.

Stoichiometrically one has the following net reactions:

*hydration of anhydride to dihydrate*

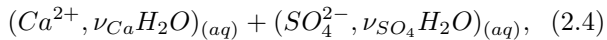
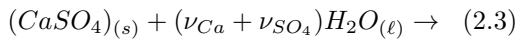


*hydration of semihydrate to dihydrate*

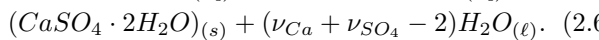
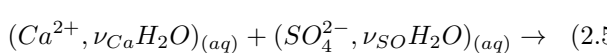


The implementation of the foregoing reactions in a reaction-diffusion model requires explicit knowledge of the dissolution/precipitation reactions, i.e., their kinetic rate equations. Observing that these rate equations are not explicitly known to us we make the following assumptions.

1. *Solubilities.* The present calciumsulphate system is strongly electrochemical. In the following we will assume nevertheless that all electrostatic interactions between solvated ions can be disregarded. Solubilities are therefore given by ionic products of concentrations. In particular,  $S_{CaSO_4}^{(\infty)} \approx 10^3 \text{ Gramm/liter} \gg S_{CaSO_4 \cdot 2H_2O} \approx 2 \text{ Gramm/liter}$ ,  $S_{CaSO_4 \cdot \frac{1}{2}H_2O} \approx 6,5 \text{ Gramm/liter}$ . All values are equilibrium values at room temperature and normal pressure. The value for  $S_{CaSO_4}^{(\infty)}$  is supposed to correspond to an infinitely high solubility.
2. *Diffusion constants.* Correspondingly we employ diffusion constants as observed for 'infinite dilution' neglecting all possible electrochemical influences. This is a simplification for liquid electrolytes. In particular,  $D^{Ca^{2+}} \approx 7.9 \cdot 10^{-10} \text{ m}^2/\text{s}$ ,  $D^{SO_4^{2-}} \approx 10.7 \cdot 10^{-10} \text{ m}^2/\text{s}$ .
3. *Solvation.* Considering the process of solvation it becomes clear that the above hydration reaction needs to be split up at least into a dissolution and a precipitation reaction. The formed ions are solvated ions *binding* a certain amount of water. Just let us write down the dissolution reaction,



and the precipitation reaction,



The numbers  $\nu_{Ca}$  and  $\nu_{SO_4}$  do characterize the formed hydrate shells of the calcium- and sulphate-Ions. One has  $\nu_{Ca} = 6$ . We are currently not aware of the value for  $\nu_{SO_4}$ . For the simulations we tentatively assume  $\nu_{SO_4} = 6$ .

4. *Specific molecular volumes.* The specific volumina of the involved solid and liquid phases under normal conditions were obtained from the literature [1], in particular:  $v_{CaSO_4} = 52.7 \cdot 10^{-3} \text{ liter/mol}$ ,  $v_{CaSO_4 \cdot 2H_2O} = 74.1 \cdot 10^{-3} \text{ liter/mol}$ ,  $v_{CaSO_4 \cdot 0.5H_2O}^{(\alpha)} = 55,7 \cdot 10^{-3} \text{ liter/mol}$ ,  $v_{CaSO_4 \cdot 0.5H_2O}^{(\beta)} = 52.7 \cdot 10^{-3} \text{ liter/mol}$  and  $v_{H_2O} = 18 \cdot 10^{-3} \text{ liter/mol}$ .
5. *Reaction constants.* The reaction constants were chosen such that firstly the back reaction of the anhydrous dissolution becomes negligibly small (irreversible reaction) and secondly the precipitation/dissolution of dihydrate is adjusted to the experimentally observed value for dihydrate solubility. For *calciumsilicates* typical scales for the involved surface reaction rates are  $10^{-6} \frac{\text{m}^4}{\text{mol} \cdot \text{s}}$ . We have tried to orientate ourselves on these magnitudes.

### III. THE MODEL

In the following we consider only the hydration of anhydrous gypsum towards dihydrate. As precise reaction mechanisms and rates are not known to us it appears reasonable to model just one dissolution and one precipitation reaction, i.e., Eqs. (2.3) and (2.5). The general model setup has been described elsewhere [8]. For the presented calculations we employed a time integration step  $\Delta t = 10^{-1} \text{ s}$  and a spatial resolution  $\Delta x = 10^{-4} \text{ m}$ . The calculations were performed in  $d = 2$  for a system of size  $100 \times 100$  and in  $d = 3$  for sizes of  $50 \times 50 \times 50$ . The dissolution rate constant was prescribed and fixed at  $k_{diss} = 10^{-3} \frac{\text{mol}}{\text{m}^2 \cdot \text{s}}$  (absolute scale) for a somewhat lower precipitation-rate-constant  $k_{prec} = 10^{-2} \cdot k_{diss}$ . The by a factor 100 lower precipitation rate constant was chosen in order to mimick the experimental observation, of a much faster dissolution than precipitation.

### IV. RESULTS

#### A. Results for $d = 2$

Fig. 1 represents the volume concentrations for anhydrous gypsum, dihydrate, and ions (left to right). Red means high - blue low concentrations.

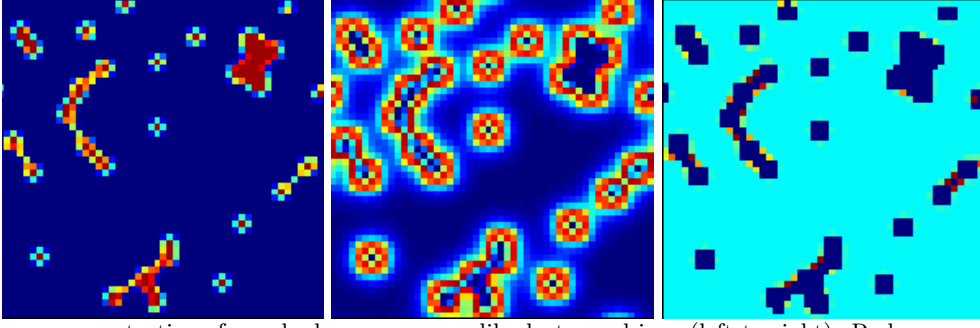


FIG. 1. Volume concentrations for anhydrous gypsum, dihydrate, and ions (left to right). Red represents high - blue low concentrations.  $k_{diss} = 10^{-3} \frac{\text{mol}}{\text{m}^2 \text{s}}$ ,  $k_{prec} = 0.1 \cdot k_{diss}$ ,  $\Delta t = 10^{-1} \text{ s}$ ,  $\Delta x = 10^{-4} \text{ m}$ ,  $L = 50$ , Time  $t = 8 \cdot 10^4 \text{ s}$ , average ion concentration  $12 \cdot 10^{-3} \frac{\text{mol}}{\text{liter}}$ .

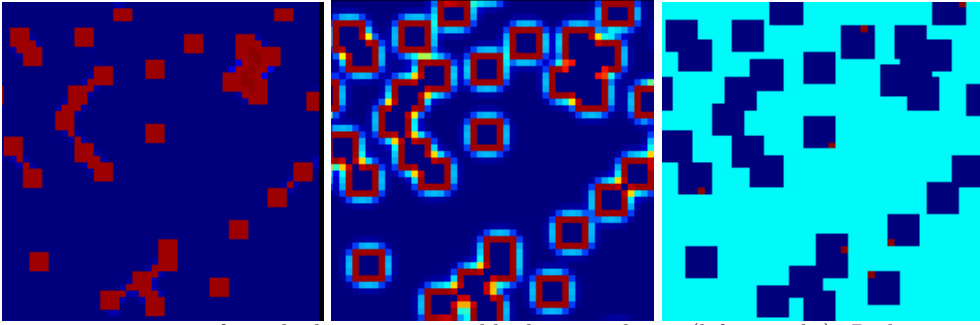


FIG. 2. Volume concentrations for anhydrous gypsum, dihydrate, and ions (left to right). Red represents high - blue low concentrations.  $k_{diss} = 10^{-3} \frac{\text{mol}}{\text{m}^2 \text{s}}$ ,  $k_{prec} = k_{diss}$ ,  $\Delta t = 10^{-1} \text{ s}$ ,  $\Delta x = 10^{-4} \text{ m}$ ,  $L = 50$ , Time  $t = 8 \cdot 10^4 \text{ s}$ , average ion concentration  $11.6 \cdot 10^{-3} \frac{\text{mol}}{\text{liter}}$ .

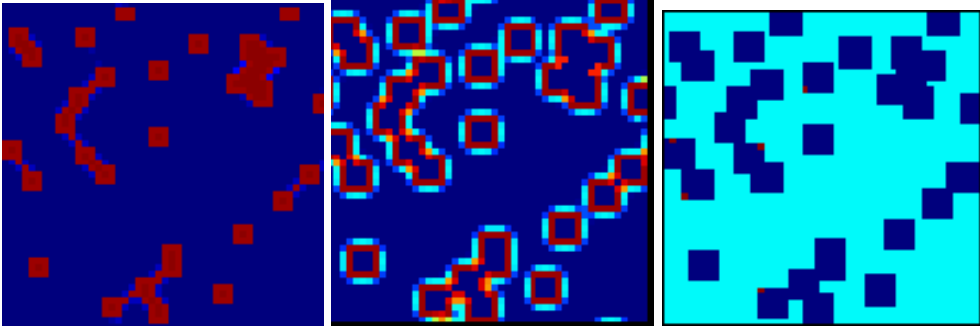


FIG. 3. Volume concentrations for anhydrous gypsum, dihydrate, and ions (left to right). Red represents high - blue low concentrations.  $k_{diss} = 10^{-3} \frac{\text{mol}}{\text{m}^2 \text{s}}$ ,  $k_{prec} = 10 \cdot k_{diss}$ ,  $\Delta t = 10^{-1} \text{ s}$ ,  $\Delta x = 10^{-4} \text{ m}$ ,  $L = 50$ , Time  $t = 8 \cdot 10^4 \text{ s}$ , average ion concentration  $11.6 \cdot 10^{-3} \frac{\text{mol}}{\text{liter}}$ .

The cases  $k_{prec} = 0.1 \cdot k_{diss}$  and  $k_{prec} = k_{diss}$  exhibit similarities where the early hydration undergoes an 'induction' period. In this induction period the ion concentrations rise steeply due to a relatively high anhydrous gypsum dissolution. After passing a maximum ion concentration the main reaction period begins to emerge in which 'outer' dihydrate starts to precipitate blocking further reactions of the anhydrid. Correspondingly ion concentrations drop to an almost stationary value, considerably slowing down the whole further hydration in the vicinity of the anhydrous gypsum grains. Such behavior is also known from calciumsilicates during the formation of inner hydrates (experimentally and numerically). The for  $k_{prec}$  over two decades almost constant ion concentration corresponds essentially to the equilibrium solubility for

drous gypsum is precipitated relatively quickly again. The velocity with which the precipitation reaction reacts with respect to the supersaturation is controlled by the rate constant  $k_{prec}$ .

In order to study the influence of the initial volume of anhydrous gypsum  $p$  on the hydration process a set of calculations was conducted. The calculations were performed for  $k_{diss} = 10^{-3} \frac{\text{mol}}{\text{m}^2 \text{s}}$  and  $k_{prec} = 10^{-2} k_{diss}$ . The basic investigated question was for which  $p$  critical percolation of the *hydrated phase* in the long run

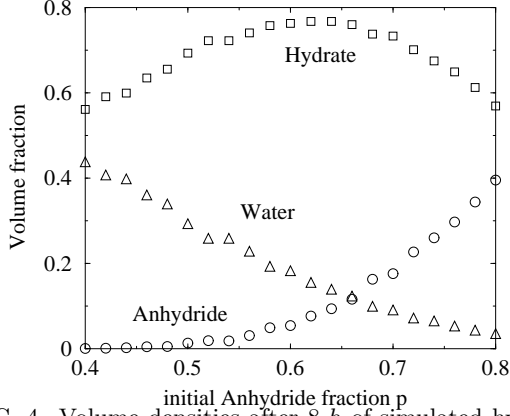


FIG. 4. Volume densities after 8 h of simulated hydration.  $k_{diss} = 10^{-3} \frac{\text{mol}}{\text{m}^2 \text{s}}$ ,  $k_{prec} = 10^{-2} k_{diss}$ ,  $L = 100$ , anhydrite ( $\circ$ ), water ( $\triangle$ ), dihydrate ( $\square$ ). All other parameters as in Fig. 1.

As a first investigation the total volume densities after eight hours of hydration time were measured in a range between  $p = 0.4$  and  $p = 0.8$ , see Figure 4. The system size was  $100 \times 100$ . The numerical effort per data point was about 40 minutes cpu time on a 2GHz PC.

For initial anhydrous gypsum densities less than  $p = 0.54$  the final remaining gypsum is less than 0.02, i.e., the dissolution reaction is complete. Above  $p = 0.6$  one observes a strongly increasing fraction of non dissolved gypsum, i.e., the reactions become increasingly incomplete. As water is not treated as

limiting reactant *per se* in the calculations there must exist a non-stoichiometric reason for the incomplete reaction. The amount of precipitated dihydrate ( $\square$ ) confirms this. The corresponding curve undergoes a maximum in reactivity for  $p$  values between 0.6 and 0.65 although sufficient amounts of water are *system wide* available. This effect is most likely due to a screening of the initial anhydrous gypsum.

Above  $p_c = 0.592$  increasingly parts of the chemically reactive interface between water and gypsum are blocked by the gypsum itself. For  $p > p_c$  one has to expect a decreasing specific surface area for the gypsum - which corresponds directly to a decreasing chemical reactivity. Let  $p$  denote the total volume fraction of initial anhydrous gypsum. As the hydrate density is a more or less continuous quantity  $\rho(x, p) \in [0, 1]$  one has to term the statement of percolation somewhat different than 'usual'. Looking at the densities  $\rho$ , we define a function  $R(x, p, r)$  with the property,

$$R(x, p, r) = \Theta(\rho(x, p) - r) \quad (4.1)$$

(with  $\Theta$  being the Heaviside step function). The function  $R(x, p, r)$  maps just all those volume elements to unity (red) for which the corresponding hydrate density exceeds a certain amount  $r$ , otherwise it becomes zero (blue). The following images show the hydrate pixels  $R(x, r)$  at  $r = 0.7$  for  $p = 0.4$ ,  $p = 0.5$ ,  $p = 0.7$ , and  $p = 0.8$  (from left to right).

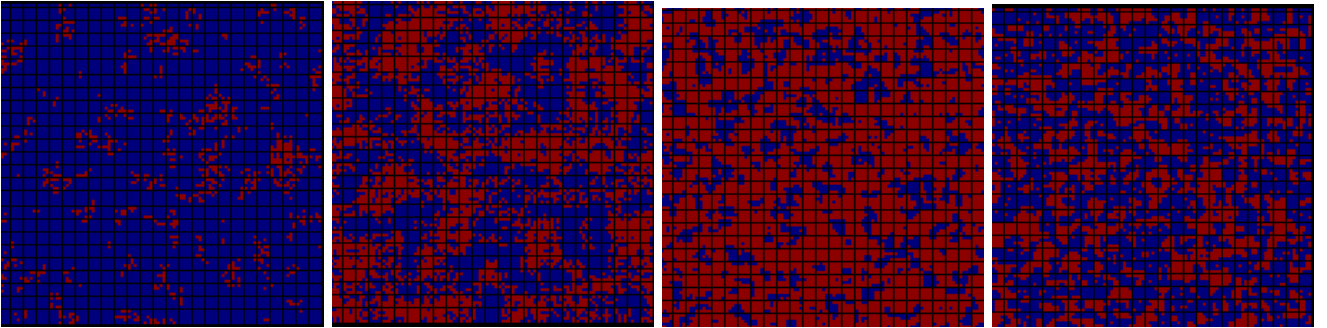


FIG. 5. Hydrate pixels at  $r = 0.7$  for initial anhydrite volume concentrations  $p = 0.4$ ,  $p = 0.5$ ,  $p = 0.7$ , and  $p = 0.8$  (from left to right). A red pixel corresponds to an asymptotic dihydrate volume concentration larger than  $r$  whereas a blue pixel represents a concentration lower than  $r$ . Parameters as in Fig. 4.

From these images it is apparent that for very high gypsum densities, i.e.,  $p = 0.8$ , the hydrate does not percolate that easily as compared for example to  $p = 0.6$ . This indicates that at least two percolation transitions for the hydrated phase do exist.

We employ volume concentrations in this work. Obviously the solid phase concentrations define a measure for the distinct properties. How to define criteria in terms of phase concentration(s) that allow an analogy to percolation phenomena? In conventional (site-)percolation each volume element is either completely occupied by species  $A$  or  $B$  at random in an *uncorrelated* way with fixed occupation probabilities  $p_A$  and  $1 - p_A$  respectively. The constant occupation

tion exhibits scale invariance (selfsimilarity) [9]. Vice versa one could employ this scale invariance as a tool in order to estimate the critical percolation probability  $p_A$ . We will follow this approach in the present paper. Because the hydrate concentrations directly correspond to non-constant occupation probabilities one could expect *correlated* percolation.

The microstructural and topological properties of the transformed phase strongly influence overall (volume) properties such as elastic properties. If -as in our case- the unreacted phase owns a small or even vanishing elastic modulus (anhydrous gypsum is usually a powder) then the percolating phase controls entirely overall properties. Therefore the percolation transition of the spatial dihydrate distribution is of central im-

question arises on how to estimate and characterize a possible percolation transition as for our case. We introduce the *typical* volume density  $r$  above which all hydrated volume elements are regarded as occupied sites in the sense of percolation. Let us denote  $k(p, r)$  as the true overall density of such sites. In general  $k(p, r)$  and  $r$  will have different values because the overall density  $k$  depends on the anhydrous volume fraction  $p$  while  $r$  is a variable. However, if we guarantee by some algorithm that the occupied sites do *always* percolate for arbitrary values of  $r$  (scales) by adjusting the initial  $p$ , then the overall density  $k$  must equal the typical density  $r$ . In other words  $k = r$  which is a fixed point of the map  $k(p, r)$ .

In order to investigate this question quantitatively more extensive calculations have been performed. One can calculate from the pixel-distribution  $R(x, p, r)$  two main quantities of interest a) its overall density,

$$k(p, r) = \frac{1}{V} \int d^3x R(x, p, r) \quad (4.2)$$

and b) the information whether *the pixel-distribution*  $R$  is percolating itself (via a burning algorithm [9]). The set of rules *without* the fixed point condition is the following:

1. Choose an initial  $r = 0.593$ ,
2. Choose a sufficient low initial gypsum density, i.e.,  $p = 0.3$  in order to find later on  $p_{min}$ .
3. Do the simulation until stationary concentration fields are reached ( here  $t = 3 \cdot 10^4$  s).
4. Calculate  $R(x, p, r)$  and  $k(p, r)$ . Determine whether  $R(x, p, r)$  is percolating or not, and choose accordingly a decremented/incremented  $p$ . A hyperbolic decreasing interval increment/decrement was chosen.
5. Continue with 3. until the increment interval becomes lower than  $\delta p = 10^{-3}$ .
6. Choose a different initial value for  $r$ , and continue with 2.

The algorithm works similar for  $p_{max}$ .

Fig. 6 shows some typical plots of hydrate densities

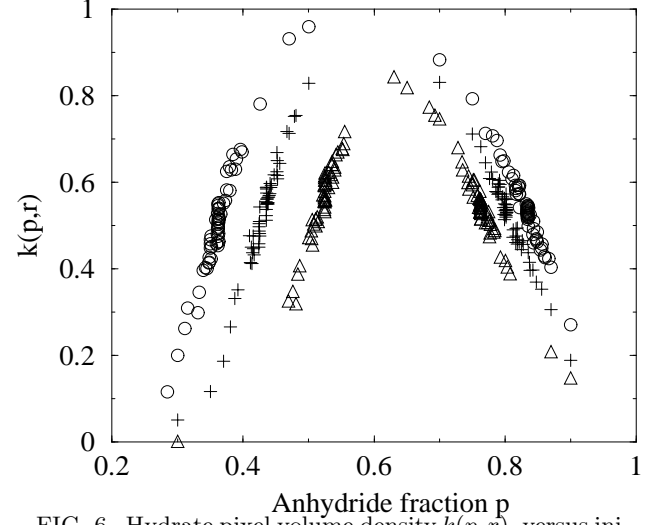


FIG. 6. Hydrate pixel volume density,  $k(p, r)$ , versus initial anhydride concentrations,  $p$ , for three different cutoffs  $r = 0.5(\circ)$ ,  $r = 0.593(+)$  and  $r = 0.7(\Delta)$ . Parameters as in Fig. 4.

The data points link the dependence of the density  $k$  and initial anhydrous volume density  $p$  for various cutoffs  $r$  under the condition that  $R$  is percolating.

It is more meaningful to average *all* points for the same  $r$  belonging to a percolating cluster, and calculate their mean and variance values, which results in one single point with error bars per value of  $r$ . This is shown in Fig. 7.

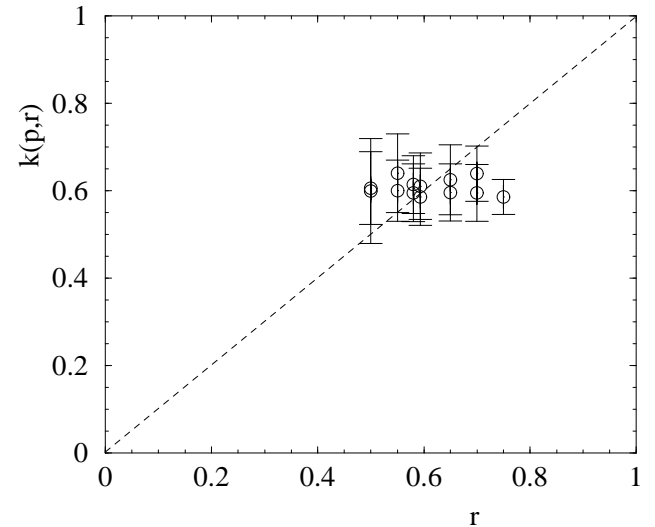


FIG. 7. Averaged hydrate pixel volume density,  $k(p_c, r)$ , versus cutoffs  $r$  for the various critical anhydride densities as observed from Fig. 6. Points that intersect the line  $k(p_c, r) = r$  define a critical value  $k_c(p_c, k_c)$ . Parameters as in Fig. 4.

We now impose the condition  $k(r, p_c) = r$  on the data points shown in Fig. 7. We find a common *critical* value  $k_c = 0.62 (+0.03 / -0.04)$ . From the lowest and highest value for  $k_c$  one obtains the desired values for the minimum and maximum percolation threshold  $p_c^{min} = 0.44 (+0.015 / -0.015)$  and  $p_c^{max} = 0.77 (+0.02 / -0.02)$ . This means in particu-

### B. Results for $d = 3$

In the foregoing paragraph we investigated a few percolation properties in  $d = 2$  depending on the initial anhydrous gypsum concentration. We found that for the case of a diluted ( $p < p_c^{min}$ ) and dense initial anhydride packing ( $p > p_c^{max}$ ) no percolation of the hydrated phase will occur, i.e. the hydrated gypsum becomes useless for most technical applications. We investigated this problem also in  $d = 3$ . To this end the reaction-diffusion model and the burning algorithm were modified.

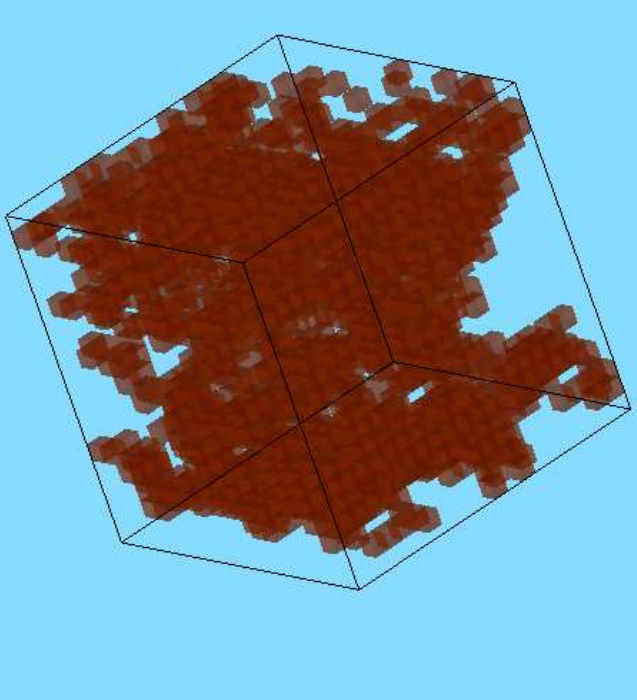


FIG. 8. A typical dihydrate backbone in  $d = 3$ , system-size  $20^3$ .

In Fig. 8 we show a small hydrate backbone, i.e. sites not belonging to a spanning cluster have been removed. One clearly sees the holes in the microstructure constituting the pore space. In order to determine the further percolation properties we employed the same numerical procedure and parameters as explained in Sec. IV A with the exception of the system size being now  $50^3$ .

The numerical effort was about 7 days CPU time

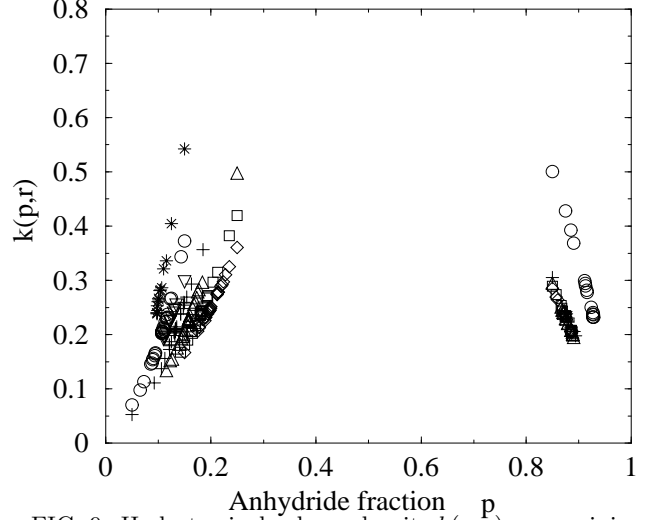


FIG. 9. Hydrate pixel volume density,  $k(p, r)$ , versus initial anhydride concentrations,  $p$ , for seven different cutoffs  $r = 0.25(\star)$ ,  $r = 0.27(o)$ ,  $r = 0.29(\nabla)$ ,  $r = 0.312(+)$ ,  $r = 0.33(\Delta)$ ,  $r = 0.35(\square)$  and  $r = 0.37(\diamond)$ . Other parameters:  $k_{diss} = 10^{-3} \frac{mol}{m^2s}$ ,  $k_{prec} = 10^{-2} k_{diss}$ ,  $L = 50$  in  $d = 3$ .

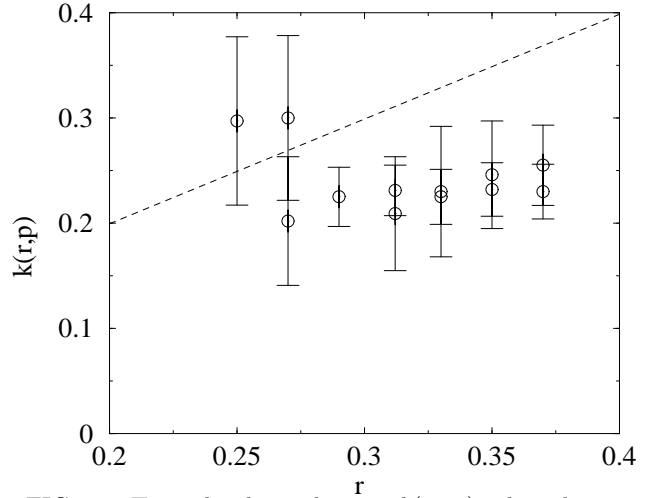


FIG. 10. Typical volume density,  $k(p_c, r)$ , plotted versus  $r$ . Points that intersect the dashed line  $k(p_c, r) = r$  define the critical  $k_c = 0.25 \pm 0.02$  in  $d = 3$ . Parameters as in Fig. 9.

The scatter of data for each  $r$  value appears much smaller than in Fig. 6. Of course are the limits for  $k(r, p \rightarrow p_c)$  smaller now, see Fig. 6, because the thresholds for uncorrelated percolation in  $d = 3$  are much smaller than in  $d = 2$ . In  $d = 3$  there exist much more connected pathways for ion diffusion and solvation. Therefore it is reasonable to expect that a possible upper percolation threshold  $p_c^{max}$  is shifted to higher anhydrous concentrations as compared to Fig. 6. Again in Fig. 10 we show mean and variance values for  $k$  versus  $r$ .

Imposing the condition  $k(r, p_c) = r$  we obtain within the error bars  $k_c = 0.25 \pm 0.02$  implying  $p_c^{min} = 0.10 \pm 0.02$  and  $p_c^{max} = 0.95 \pm 0.02$ . As  $p_c^{max}$  is very high compared to  $d = 2$  this could play a cer-

## V. CONCLUSION

We studied percolation properties of a reaction-diffusion model for the hydration of calciumsulphate. From a kinetic point of view the basic effects of the dissolving and precipitating microstructures are a) that they control the ion diffusion transport to a large extent and b) that they form a spanning backbone from one systems end to the other, thus allowing the transport of momentum/stress.

We expect that for  $p < p_c^{min}$  and  $p > p_c^{max}$  microstructures are unable to carry stress at all. It should be noted that for  $d = 2$  and  $d = 3$   $p_c^{max}$  is not reachable employing mono-disperse packings.

Our results also show that there exists an optimum initial anhydrous concentration for which the total amount of dihydrate reaches a maximum, i.e. shows maximum overall chemical reactivity, and possibly the best mechanical properties.

The relatively high computing time for  $d = 3$  indicates that one possibly should consider in the future a different evaluation method than exact enumeration in order to solve the reaction-diffusion equations.

- 
- [1] F. Wirsching, *Calcium Sulphate* in Ullmann's Encyclopedia of Industrial Chemistry, 6th Edition, (1998).
  - [2] *Cement Chemistry*, H. F. W. Taylor, Academic Press, 1990.
  - [3] Kuzel and Hauner, *Zement Kalk Gips* **40**, 628-32 (1987).
  - [4] A. J. Lewry and J. Williamson, *J. Mat. Sci.* **29**, 5279-84, (1994). A. J. Lewry and J. Williamson, *J. Mat. Sci.* **29**, 5524-28, (1994) A. J. Lewry and J. Williamson, *J. Mat. Sci.* **29**, 6085-90, (1994).
  - [5] D. P. Bentz and E. J. Garboczi, *Percolation of phases in a three-dimensional cement paste microstructural model*, Cement and Concrete Research, vol. **21**, 325-44 (1991).
  - [6] D. P. Bentz, P. V. Coveney, E. J. Garboczi, M. F. Kleyn and P. E. Stutzman, *Cellular automaton simulations of cement hydration and microstructure development*, Modelling Simul. Mater. Sci. Eng. **2**, 783-808 (1994).
  - [7] B. Madé, A. Clément and B. Fritz, *Modélisation thermodynamique et cinétique des réactions diagénétiques dans les bassins sédimentaires*, Revue de L'institut français du pétrole **49** (6), (1994).
  - [8] F. Tzschichholz, H.J. Herrmann and H. Zanni, *Reaction-diffusion model for the hydration and setting of cement*, Phys. Rev. **E 53**, (3), 2629-37 (1996).
  - [9] D. Stauffer, Introduction to Percolation Theory (Taylor and Francis, London, 1985).
  - [10] H. Scholze, M. Hurbaniac and H. Ruf, *Comperative considerations on the behaviour of natural gypsum and flue gas gypsum*, Zement-Kalk-Gips 10, (1985).